Journal of the Ceramic Society of Japan 122 [2] 141-145 2014 Paper

Protective effect of CeO_2 nanoparticles on photo-induced oxidative damage of DNA

Naoko FUJITA and Kai KAMADA†

Department of Materials Science and Engineering, Faculty of Engineering, Nagasaki University, 1–14 Bunkyo-machi, Nagasaki 852–8521, Japan

The present paper demonstrates that inorganic ceria (CeO_2) nanoparticles effectively inhibit anomalous oxidative damage of DNA induced by ultraviolet (UV) light irradiation. To utilize the CeO_2 nanoparticles for the protection test of DNA, a colloidal solution of monodispersed and crystallized CeO_2 nanoparticles is synthesized through a photochemical reaction of $Ce(NO_3)_3$ solution, followed by dialysis to remove unreacted electrolytes. Subsequently, the UV light induced oxidative damage of DNA in the presence or absence of CeO_2 nanoparticles is evaluated by a quantitative analysis of 8-hydroxy-2′-deoxyguanosine (8-OHdG) which is an oxidation product of guanine in base sequences. The 8-OHdG concentration in DNA is increased by the exposure to UV light. On the other hand, the co-presence of CeO_2 nanoparticles diminish the formation rate of 8-OHdG. Such favorable effect of CeO_2 nanoparticles is due to an excellent annihilation activity of reactive oxygen species (ROS) accounting for the DNA oxidation as well as a UV light absorption ability based on semiconducting nature.

Key-words : Oxide nanoparticle, Radical annihilation, Anti-oxidation, Enzyme-mimetic activity

[Received November 5, 2013; Accepted December 5, 2013]

1. Introduction

As well-known, DNA damages originated from oxidation of nucleobases induce mutation and/or inhibition of genetic information transfer, followed by contraction of various diseases. For example, reactive oxygen species (ROS) generated through an electron transport chain in mitochondrion or under a high-energy radiation (ultraviolet ray, X-ray) bring about the serious oxidative stress of DNA. Therefore, organisms possess multiple biological defense systems against the stresses such as ROS level control by redox enzymes or presence of DNA repair enzymes. Recently, it has been reported that inorganic nanoparticles including noble metals and elementary calcogens are effective for annihilation of various ROS (superoxide anion radical, singlet oxygen, hydrogen peroxide, etc.).[1)–4)] In other words, these inorganic nanoparticles show enzyme-mimetic activities beneficial to the biological defense. In addition to the precious single elements, several metal oxide nanoparticles are also potent to annihilate the ROS.[5)–7)] However, the ROS scavenging mechanism by the inorganic nanoparticles is less clarified at present. Seal and coworkers claimed that ceria (CeO_2) nanoparticles were useful for protection of normal cells against radiation-induced damages[8)–10)] and reduction of ROS level in vitro.[11)–13)] These facts imply that the CeO_2 nanoparticle is promising as a novel inorganic anti-oxidant to avoid the excess ROS evolution incurring the oxidative DNA degeneration.

We have recently developed a novel technique to prepare an aqueous CeO_2 sol via a photochemical reaction of $Ce(NO_3)_3$ solution.[14)] Since the photo-irradiation causes a homogeneous reaction over the entire solution, monodispersed and crystallized CeO_2 nanoparticles are formed without any heat treatment that frequently leads to aggregation or undesired grain growth. Furthermore, a purified aqueous CeO_2 sol is easily obtained by dialysis of the solution against doubly distilled water to remove unreacted solutes. To reveal an effectiveness of photochemically produced aqueous CeO_2 sol for the biological defense system, influences on UV light-induced oxidative damage of DNA are described in the present paper. As stated already, DNA is injured by direct interaction with UV light, and undergoes hydroxylation, deamination, and dimerization of pyrimidines.[15)] Alternatively, ROS generated from dissolved oxygen receiving a photon energy lead to indirect photo-oxidation of DNA.[16)–18)] The photo-oxidative damage by irradiating UV-B (wavelength region: 320–280 nm) or UV-C (280–100 nm) is suppressed in the presence of flavonoids[19),20)] or polyphenols[21)–23)] as ROS scavengers. In contrast, the co-existence of photosensitizers such as methylene blue or riboflavin stimulates the DNA oxidation even under UV-A (380–320 nm) or visible light irradiation with a relatively moderate energy.[24)] On the other hand, there are few previous papers describing the effect of inorganic nanoparticles on the photo-oxidative damage of DNA within our knowledge. As an only example, Hidaka et al. have reported that photo-deformation of DNA plasmids depends on photocatalytic activity of coexisted oxide semiconductors (ZnO, TiO_2, CeO_2).[25)] They confirmed that the undoped and doped CeO_2 had little influence on the DNA damage, but the defensive action of CeO_2 was not mentioned. The present paper demonstrates that the photochemically produced CeO_2 nanoparticles effectively reduce the oxidation rate of DNA due both to the ROS scavenging and UV-light shielding abilities.

2. Experimental procedure

2.1 Synthesis of aqueous ceria sol via photochemical reaction

The photochemical synthesis of CeO_2 nanoparticles was carried out by a procedure noted in our previous paper with minor modifications.[14)] Briefly, an aqueous $Ce(NO_3)_3$ solution (11.4 mM) including 6-aminohexanoic acid (AHA, 90.9 mM)

† Corresponding author: K. Kamada; E-mail: kkamadda@nagasaki-u.ac.jp

DOI http://dx.doi.org/10.2109/jcersj2.122.141

was adjusted to pH 5.5 by addition of a minute amount of 1 M HCl, and then was exposed to a UV light from 500 W high pressure mercury lamp at 293 K for 4 h. After the reaction, the purified aqueous CeO_2 sol was obtained by dialysis against doubly distilled water using membrane filter (MWCO: 3000) to remove the electrolytes remained. Distribution state and average diameter of the CeO_2 nanoparticles were analyzed through a dynamic light scattering (DLS) technique. CeO_2 content in the resultant aqueous sol was estimated using an inductively coupled plasma (ICP) analysis. UV–visible absorption spectrum of the CeO_2 sol was measured by a spectrophotometer. Crystal structure and morphology of the dried product were analyzed using a Raman spectroscopy and a transmission electron microscopy (TEM), respectively. An X-ray photoelectron spectroscopy (XPS) was employed to determine oxidation state of the CeO_2 surface.

2.2 Annihilation of superoxide anion radicals

DNA oxidation is significantly accelerated in the presence of ROS, and hence ROS scavenging activity of CeO_2 nanoparticles was also studied for superoxide anion radical ($\bullet O_2^-$) and compared with a naturally occurring enzyme (CuZn-SOD, superoxide dismutase, 32 kDa). The $\bullet O_2^-$ was generated using a hypoxanthine (HX)/xanthine oxidase (XOD) reaction system. Cytochrome c is reduced by the $\bullet O_2^-$ and then gives rise to a rapid increment of absorbance at 550 nm (A_{550}).[26] Therefore, variation in A_{550} after injection of 0.72 mM HX (20 µl) to mixed solution of the scavenger (CeO_2 or SOD, 10 µl), XOD (61 mU/ml, 10 µl), and cytochrome c (0.24 mM, 10 µl) in 0.1 M PBS dissolving 0.05 mM EDTA (pH 7.5, 150 µl) was recorded using a microplate reader for 3 min at 310 K. In this paper, the identical PBS was used as a medium for all experiments unless otherwise stated. Taking into account a linear proportion of initial slope of A_{550} to the $\bullet O_2^-$ concentration, the $\bullet O_2^-$ scavenging activity was defined as a decreasing ratio of the slope for the scavenger-free solution. On the other hand, H_2O_2 produced by the quenching of $\bullet O_2^-$ was quantified by means of peroxidase assay. An aliquot of solution (48 µl) after the radical scavenging reaction without the cytochrome c was mixed with the PBS (2352 µl) including horseradish peroxidase (HRP, 20 mU/ml) and guaiacol (1 mM), then a maximum absorbance (470 nm) derived from polymeric oxidation product of guaiacol[27] was measured after incubation for 2.5 min at 298 K. The H_2O_2 concentration was calculated with a calibration curve fabricated using standard H_2O_2 solutions in advance.

2.3 Evaluation of UV light-induced DNA damage

The effect of CeO_2 nanoparticles on the photo-induced oxidative damage of DNA was examined as follows. Double-stranded DNA sodium salts from salmon testes (ca. 2 kbp) were dissolved in the PBS (2 mg/ml). The DNA solution (500 µl) including or excluding the CeO_2 nanoparticles in a quartz glass cell was exposed to a UV light (300 W Hg-Xe lamp) at 303 K for a certain period. Since guanine in base sequences is oxidized to 8-hydroxy-2′-deoxyguanosine (8-OHdG, oxidation marker) by the photoirradiation, the 8-OHdG concentration after the irradiation was quantitatively estimated through a competitive enzyme-linked immunosorbent assay (ELISA).[28]

3. Results and discussion

3.1 Photochemical synthesis of CeO_2 nanoparticles

UV light irradiation to a colorless and transparent $Ce(NO_3)_3$ aqueous solution at pH 5.5 caused a formation of pale yellowish colloidal solution. In our previous paper,[14] it has been revealed that the NO_3^- oxidizes the Ce^{3+} under the UV light illumination, then the Ce^{4+} with a lower solubility than the reduced form is immediately precipitated as a hydrated CeO_2 nanoparticle. 6-aminohexanoic acid (AHA, $pKa_1 = 4.4$, $pKa_2 = 10.8$) added as a dispersant has positive and negative charges on N- and C-terminuses at pH 5.5, respectively. Hence, the C-terminus (carboxyl ion) of AHA could be electrostatically adsorbed on the positive CeO_2 surface with an isoelectric point at pH∼6.[29] In fact, the pale yellowish appearance of sol is a sign of the coordination of carboxyl groups to the surface Ce ion,[30] and moreover, a colorless sol was obtained in an AHA-free solution. As a result of the AHA adsorption, the electrostatic repulsion between the opposite amino groups disturbs excessive coagulation of the CeO_2 nanoparticles in the medium. The facts that the particle size distribution curve of the aqueous CeO_2 sol is composed of a single peak and the mean diameter of CeO_2 nanoparticles was about 14 nm as shown in **Fig. 1**, suggests that the photochemical reaction forms the monodispersed and stable colloidal solution.

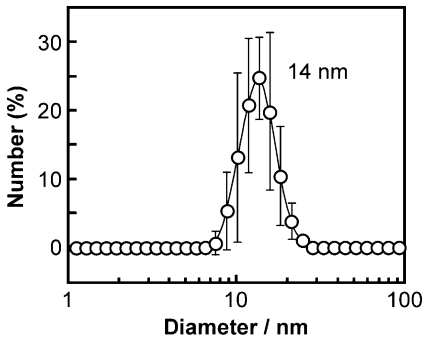

Fig. 1. Particle size distribution of CeO_2 nanoparticles synthesized by UV light irradiation to 11.4 mM $Ce(NO_3)_3$ + 90.9 mM AHA (pH 5.5) for 4 h at 293 K.

Figure 2 displays the TEM image and the Raman spectrum of powder after drying the sol at an ambient condition. In the TEM image [Fig. 2(a)], clear lattice fringes are observed in each particle. A primary particle size is estimated to be 3–5 nm, indicating that a few CeO_2 nanoparticles are aggregated in the aqueous sol (∼14 nm). The Raman spectrum [Fig. 2(b)] exhibited two bands. The larger peak at 467 cm^{-1} corresponds to a triply degenerate Raman active F_{2g} mode of fluorite structure, which is detected as a symmetric breathing mode of the oxygen atoms surrounding cations.[31),32] The small and broad peak at the larger Raman shift (around 600 cm^{-1}) is related to oxygen defects produced by partial reduction of Ce^{4+}, that is, CeO_{2-x}. Consequently, it can be concluded that the photochemical reaction of the AHA-added $Ce(NO_3)_3$ solution results in the formation of stable and crystallized CeO_2 nanoparticles with the monodispersed size distribution.

3.2 Radical annihilation performance of CeO_2 nanoparticles

Since the photo-induced damage of DNA is closely concerned with the ROS, evaluation of ROS scavenging activity of the CeO_2 nanoparticles will help us to understand the protective performance. Hence, the annihilation of superoxide anion radical ($\bullet O_2^-$) by the CeO_2 nanoparticles was assessed and compared with enzyme CuZn-SOD. The dependence of scavenger (CeO_2 or SOD) concentration on the $\bullet O_2^-$ quenching is shown in **Fig. 3**(a). In this figure, the CeO_2 dose is described as "particle concen-

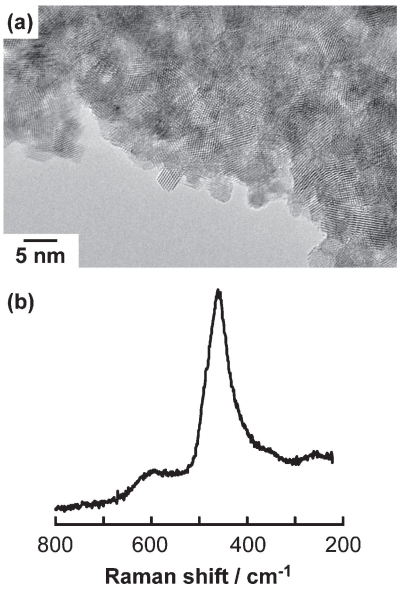

Fig. 2. (a) TEM image and (b) Raman spectrum of CeO_2 nanoparticles after drying aqueous sol at room temperature.

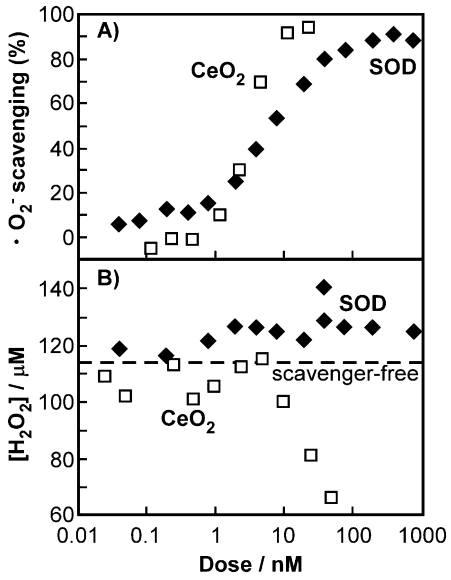

Fig. 3. (a) Dose-dependent $\bullet O_2^-$ scavenging activity of CeO_2 nanoparticles and CuZn-SOD. (b) H_2O_2 concentration of mixed solution after $\bullet O_2^-$ scavenging reaction.

tration" calculated on the assumption that all CeO_2 nanoparticles have a spherical shape and an identical diameter (14 nm). In addition to the SOD, the CeO_2 nanoparticles also had a dose-dependent $\bullet O_2^-$ scavenging activity, confirming the SOD-mimetic activity of CeO_2 nanoparticles. According to non-linear regressions of the data in Fig. 3(a), the 50% inhibitory concentration (IC_{50}) of CeO_2 and SOD was roughly estimated to be about 3.2 and 7.0 nM, respectively. The result means that the CeO_2 nanoparticles have more superior activity (2.2 times) than the SOD. Furthermore, the measured activity was almost comparable to that of CeO_2 nanoparticles prepared by a wet chemical method and subsequent hydrothermal treatment (ca. 2–3 times larger than the CuZn-SOD).[11] In order to investigate the influence of cohesiveness on the SOD-mimetic activity, the O_2^- scavenging performance of the aqueous CeO_2 sol was evaluated after hydrothermal treatment at 373 K for 3 h. The mean diameter was increased to 126 nm by the heat-treatment, implying the agglomeration of the nanoparticles. It was revealed that the heat-treated CeO_2 sol has little SOD-mimetic activity. The deterioration in the activity would be explained by the reduced specific surface area. Consequently, it was confirmed that the proposed photochemical synthesis accomplished the formation of CeO_2 nanoparticles as prominent artificial SOD mimics without any heat treatment. The high performance of photochemically produced CeO_2 nanoparticles should be related to the well-dispersion in the medium.

Typically, the enzyme SOD catalyzes dismutation of $\bullet O_2^-$ to O_2 and H_2O_2 accompanied by a valence change of transition metal ions (Cu, Mn, etc.) in active centers. Thus, the redox potential of metal ion should exist an intermediate position between the electrochemical couples of $\bullet O_2^-/H_2O_2$ and $\bullet O_2^-/O_2$ to dismutate efficiently. Because the CeO_2 nanoparticles have the mixed valence state as stated above, the O_2^- scavenging on the CeO_2 surface seems to proceed as both or one of following reactions:[11),33)]

$$Ce^{4+} + \bullet O_2^- \rightarrow Ce^{3+} + O_2 \text{ (Oxidation)} \quad (1)$$

$$Ce^{3+} + \bullet O_2^- + 2H^+ \rightarrow Ce^{4+} + H_2O_2 \text{ (Reduction)} \quad (2)$$

The previous paper has reported that a highly reduced CeO_2 surface (that is, high Ce^{3+} concentration) achieves a better scavenging performance.[11] However, the standard solid-state redox potential of $Ce^{IV}O_2/Ce^{III}(OH)_3$ ($E^o = +1.56$ V vs. NHE)[34] is considerably positive than both potentials of $\bullet O_2^-/H_2O_2$ (+0.90 V) and $\bullet O_2^-/O_2$ (−0.33 V),[35] suggesting that the oxidation route by the Ce^{4+} [Eq. (1)] is thermodynamically favored, whereas the reduction by the Ce^{3+} is impossible. Figure 3(b) plots the H_2O_2 concentration in the test solution after the scavenging reaction. The generated $\bullet O_2^-$ (lifetime: several seconds in neutral∼basic media) was spontaneously disproportionated into H_2O_2 and O_2 even in the scavenger-free solution, and a certain level of H_2O_2 was produced (dashed line, 114 μM). The scavenging reaction by the SOD led to a minor increase in the H_2O_2 concentration independent of the SOD dose. In contrast, the addition of a large amount of CeO_2 drastically reduced the H_2O_2 concentration especially at more than 10 nM that corresponded to a sufficient concentration for the complete O_2^- annihilation. This result implies that the Ce^{4+} [Eq. (1)] rather than the Ce^{3+} [Eq. (2)] tends to participate in the $\bullet O_2^-$ scavenging reaction. Actually, $Ce^{3+}/(Ce^{3+} + Ce^{4+})$ molar ratio in the CeO_2 surface analyzed by X-ray photoelectron spectroscopy gained by the reaction (17 → 31%). On the other hand, these results cannot deny that the decline of H_2O_2 concentration at the higher doses is caused by a catalase-mimetic activity of CeO_2 previously demonstrated.[13] Consequently, it is predicted that the present CeO_2 nanoparticles effectively annihilate the $\bullet O_2^-$ and hence are applicable as protective agents against the photo-induced oxidation of DNA.

3.3 Inhibition of photo-induced oxidative damage of DNA under co-presence of CeO_2 nanoparticles

The influence of CeO_2 nanoparticles on the UV light-induced oxidative damage of DNA was examined. The degree of oxidative damage was evaluated by a quantitative analysis of 8-OHdG which is oxidation product of guanine with most negative oxidation potential among four primary nucleobases.[36)–38)] **Figure 4**(a) summarizes the 8-OHdG concentrations in the DNA solution after incubating under various conditions at pH 7.5 and 303 K.

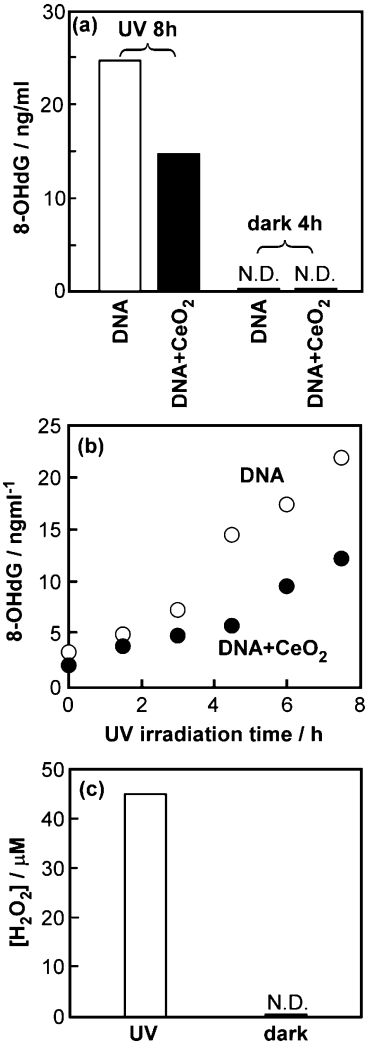

Fig. 4. (a) Influence of CeO_2 nanoparticles (12.0 nM) on 8-OHdG concentration in DNA (2 mg/ml, pH 7.5) after UV light irradiation at 303 K. (b) Variation in 8-OHdG concentration of DNA solution (2 mg/ml, pH 7.5) during UV light irradiation in the presence or absence of CeO_2 nanoparticles (12.0 nM). (c) H_2O_2 concentration in DNA solution after UV light irradiation or incubation in the dark for 8 h.

In the dark state, no formation of 8-OHdG was detected irrespective of the presence of CeO_2 nanoparticles, supporting that the DNA was not affected by a simple contact with the nanoparticles. The UV light irradiation caused a viscosity lowering of the DNA solution owing to fragmentations, and increased the 8-OHdG concentration. In contrast, the co-existence of CeO_2 nanoparticles diminished the concentration by 40%. The inhibitory effect of CeO_2 nanoparticles was remarkable especially at a longer irradiation time [Fig. 4(b)]. These results indicate that the CeO_2 nanoparticles are useful for protecting the photo-induced oxidative damage of DNA.

It is believed that highly aggressive hydroxyl radicals (•OH) produced by UV radiation to dissolved oxygen are responsible for non-specific oxidation of DNA.[15] Wei et al. have reported that an 8-OHdG concentration in a calf thymus DNA solution under UV-C radiation is increased in proportion to irradiation time and intensity.[17),18] They explained that energy transfer from the triplet state of irradiated thymine to dissolved oxygen formed singlet oxygen ($^1O_2$) accounting for specific oxidation of guanine. The photo-induced DNA oxidation in the present study was

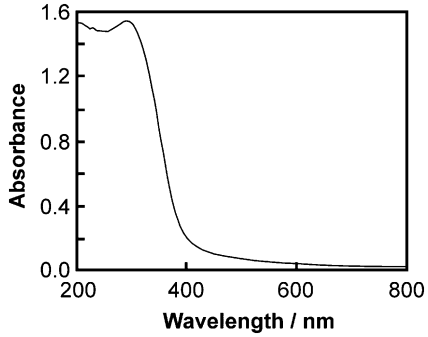

Fig. 5. UV–vis absorption spectrum of photochemically produced aqueous CeO_2 sol (452 nM, pH 7.5).

anticipated to proceed through these mechanisms. For instance, the $\bullet O_2^-$ derived from dissolved oxygen is transformed into H_2O_2, and then the H_2O_2 is photochemically decomposed into the hydroxyl radicals ($O_2 \rightarrow \bullet O_2^- \rightarrow H_2O_2 \rightarrow$ •OH). Finally, the hydroxyl radicals non-specifically oxidize the nucleobases. In fact, an enhancement of H_2O_2 level in the DNA solution under the UV light irradiation was confirmed [Fig. 4(c)].

The protective effect of CeO_2 nanoparticles depicted in Fig. 4 would be attributed to following two factors. One is the ROS scavenging activity of the CeO_2 nanoparticles as demonstrated in Fig. 3(a). That is, since the CeO_2 nanoparticles annihilate the $\bullet O_2^-$ which is the intermediate of hydroxyl radical, the addition of CeO_2 sol will diminish a radical concentration during the UV light illumination. The preferential conversion of $\bullet O_2^-$ to O_2 rather than aggressive H_2O_2 [Fig. 3(b)] may be also favorable to suppress the DNA damage. Another factor is a semiconducting nature of CeO_2. Cubic fluorite CeO_2 behaves as an n-type semiconductor with a band gap energy of 3.2 eV equivalent to wavelength of UV-A (<388 nm).[30),39),40] In fact, the prepared CeO_2 sol can absorb the UV light with wavelengths shorter than ca. 400 nm as shown in **Fig. 5**. Furthermore, the photocatalytic oxidation activity of CeO_2 is typically much less than those of other semiconductors such as ZnO and TiO_2.[28] Therefore, the CeO_2 nanoparticles can reflect or absorb the incident UV light and thus retard the photochemical reaction of dissolved oxygen and/or DNA. Whereas the activity of naturally occurring enzymes such as SOD and catalase is deteriorated by exposure to the UV light, the inorganic CeO_2 nanoparticles appear to be quite stable. Judging from these facts, it is concluded that the CeO_2 nanoparticles with the SOD-mimetic activity have a practical protective effect on the photo-induced oxidative damage of DNA.

4. Conclusions

In the present study, the aqueous CeO_2 sol was fabricated by the photochemical technique, and the influence of CeO_2 sol addition on the formation of oxidized DNA under the UV light irradiation was clarified. The photochemical reaction of $Ce(NO_3)_3$ solution achieved the production of monodispersed and crystallized CeO_2 colloidal solution without any heat treatment. The obtained CeO_2 nanoparticles showed a similar $\bullet O_2^-$ annihilation performance to the enzyme SOD on the basis of the valence fluctuation of Ce ions, and the activity exceeded that of the SOD. The radical scavenging activity depended on the oxidation state of CeO_2 surface, and the tetravalent Ce ions mainly caused the $\bullet O_2^-$ quenching. The UV light-induced oxidation of DNA was tested by the quantitative analysis of 8-OHdG as an oxidation marker. The co-presence of CeO_2 nanoparticles remarkably inhibited the progress of photo-induced oxidative

damage of DNA. The favorable effect was based on the radical scavenging and the UV light absorption property of CeO_2 nanoparticles. It is supposed that the aqueous sol is appropriate for some biochemical applications such as UV-screening cosmetics[25),30)] and enzymatic replacement therapy,[4)] because the utilization of sol easily realizes a precise adjustment of administration concentration as compared with powder sample. In order to enhance the protecting effect of CeO_2 nanoparticles, morphology, and doping of different cations on the photo-induced DNA damage including fragmentation and deformation will be investigated in the near future. Needless to say, toxicology studies of the nanoparticles should be also undertaken to evaluate their safety regarding various biochemical applications.[41)–44)]

References

1) W. He, Y. Liu, J. Yuan, J.-J. Yin, X. Wu, X. Hu, K. Zhang, J. Liu, C. Chen, Y. Ji and Y. Guo, *Biomaterials*, **32**, 1139–1147 (2011).
2) J. Fan, J.-J. Yin, B. Ning, X. Wu, Y. Hu, M. Ferrari, G. J. Anderson, J. Wei, Y. Zhao and J. Nie, *Biomaterials*, **32**, 1611–1618 (2011).
3) B. Huang, J. Zhang, J. Hou and C. Chen, *Free Radic. Biol. Med.*, **35**, 805–813 (2003).
4) A. Clark, A. Zhu, K. Sun and H. R. Petty, *J. Nanopart. Res.*, **13**, 5547–5555 (2011).
5) J. P. Saikia, S. Paul, B. K. Kowar and S. K. Samdarshi, *Colloids Surf., B*, **78**, 146–148 (2010).
6) J. P. Saikia, S. Paul, B. K. Kowar and S. K. Samdarshi, *Colloids Surf., B*, **79**, 521–523 (2010).
7) S. Paul, J. P. Saikia, S. K. Samdarshi and B. K. Kowar, *J. Magn. Magn. Mater.*, **321**, 3621–3623 (2009).
8) J. Chen, S. Patil, S. Seal and J. F. McGinnis, *Nat. Nanotechnol.*, **1**, 142–150 (2006).
9) J. Colon, N. Hsieh, A. Ferguson, P. Kupelian, S. Seal, D. W. Jenkins and C. H. Baker, *Nanomedicine*, **6**, 698–705 (2010).
10) R. W. Tarnuzzer, J. Colon, S. Patil and S. Seal, *Nano Lett.*, **5**, 2573–2577 (2005).
11) C. Korsvik, S. Patil, S. Seal and W. T. Self, *Chem. Commun.*, 1056–1058 (2007).
12) E. G. Heckert, A. S. Karakoti, S. Seal and W. T. Self, *Biomaterials*, **29**, 2705–2709 (2008).
13) T. Pirmohamed, J. M. Dowding, S. Singh, B. Wasserman, E. Heckert, A. S. Karakoti, J. E. S. King, S. Seal and W. T. Self, *Chem. Commun.*, **46**, 2736–2738 (2010).
14) K. Kamada, K. Horiguchi, T. Hyodo and Y. Shimizu, *Cryst. Growth Des.*, **11**, 1202–1207 (2011).
15) C. Kielbassa, L. Roza and B. Epe, *Carcinogenesis*, **18**, 811–816 (1997).
16) G. P. Pfeifer and A. Besaratinia, *Photochem. Photobiol. Sci.*, **11**, 90–97 (2012).
17) H. Wei, Q. Ca, R. Rahn, X. Zhang, Y. Wang and M. Lebwohl, *Biochemistry*, **37**, 6485–6490 (1998).
18) H. Wei, Q. Cai, R. Rahn and X. Zhang, *Free Radic. Biol. Med.*, **23**, 148–154 (1997).
19) L. F. Yamaguchi, M. J. Kato and P. D. Mascio, *Phytochemistry*, **70**, 615–620 (2009).
20) L.-O. Klotz and H. Sies, *Toxicol. Lett.*, **140–141**, 125–132 (2003).
21) D. Rivero, S. Pérez-Magariño, M. L. González-Sanjosé, V. Valls-Belles, P. Codoñer and P. Muñiz, *J. Agric. Food Chem.*, **53**, 3637–3642 (2005).
22) G. Nie, T. Wei, S. Shen and B. Zhao, *Methods Enzymol.*, **335**, 232–244 (2001).
23) S. K. Katiyar, F. Afaq, A. Perez and H. Mukhtar, *Carcinogenesis*, **22**, 287–294 (2001).
24) S. Y. Kim, E. J. Kim and J.-W. Park, *J. Biochem. Mol. Biol.*, **35**, 353–357 (2002).
25) H. Hidaka, H. Kobayashi, T. Koike, T. Sato and N. Serpone, *J. Oleo Sci.*, **55**, 249–261 (2006).
26) H. J. Forman and I. Fridovich, *Arch. Biochem. Biophys.*, **158**, 396–400 (1973).
27) H. Tonami, H. Uyama, R. Nagahata and S. Kobayashi, *Chem. Lett.*, **33**, 796–797 (2004).
28) C.-C. Chiou, P.-Y. Chang, E.-Ch. Chan, T.-L. Wu, K.-C. Tsao and J.-T. Wu, *Clin. Chim. Acta*, **334**, 87–94 (2003).
29) P. Suphantharida and K. Osseo-Assare, *J. Electrochem. Soc.*, **151**, G658–G662 (2004).
30) T. Masui, H. Hirai, R. Hamada, N. Imanaka, G.-Y. Adachi, T. Sakata and H. Mori, *J. Mater. Chem.*, **13**, 622–627 (2003).
31) I. Kosacki, T. Suzuki, H. U. Anderson and P. Colomban, *Solid State Ionics*, **149**, 99–105 (2002).
32) G.-R. Li, D.-L. Qu, L. Arurault and Y.-X. Tong, *J. Phys. Chem. C*, **113**, 1235–1241 (2009).
33) C. Ispas, J. Njagi, M. Cates and S. Andreescu, *J. Electrochem. Soc.*, **155**, F169–F176 (2008).
34) M. Pourbaix, "Atlas of Electrochemical Equilibria in Aqueous Solutions", National Association of Corrosion Engineers: Houston (1974).
35) M. Yuasa, K. Oyaizu, A. Ogata, N. Matsukura and A. Yamaguchi, *J. Oleo Sci.*, **554**, 233–239 (2005).
36) S. Steenken and S. V. Jovanovic, *J. Am. Chem. Soc.*, **119**, 617–618 (1997).
37) D. H. Johnston, C.-C. Cheng, K. J. Campbell and H. H. Thorp, *Inorg. Chem.*, **33**, 6388–6390 (1994).
38) M. D. Evans, M. S. Cooke, I. D. Podmore, Q. Zheng, K. E. Herbert and J. Lunec, *Biochem. Biophys. Res. Commun.*, **254**, 374–378 (1999).
39) T. Sato, T. Katakura, S. Yin, T. Fujimoto and S. Yabe, *Solid State Ionics*, **72**, 377–382 (2004).
40) K. Kamada, J.-H. Kang, S.-M. Park and J.-H. Choy, *J. Phys. Chem. Solids*, **73**, 1478–1482 (2012).
41) I. Celardo, M. D. Nicola, C. Mandoli, J. Z. Pedersen, E. Traversa and L. Ghibelli, *ACS Nano*, **5**, 4537–4549 (2011).
42) R. Wan, Y. Mo, L. Feng, S. Chien, D. J. Tollerud and Q. Zhang, *Chem. Res. Toxicol.*, **25**, 1402–1411 (2012).
43) E. Girgis, W. K. B. Khalil, A. N. Eman, M. B. Mohamed and K. V. Rao, *Chem. Res. Toxicol.*, **25**, 1086–1098 (2012).
44) G. P. Jose, S. Santra, S. K. Manal and T. K. Sengupta, *J. Nanobiotechnology*, **9**, 9 (2011).